Nuclear magnetic resonance in the antiferromagnetic heavy-fermion system UCu_5: spin reorientation at 1 K

1994 J. Phys.: Condens. Matter 6 10567

(http://iopscience.iop.org/0953-8984/6/48/017)

J. Phys.: Condens. Matter 6 (1994) 10567–10592. Printed in the UK

Nuclear magnetic resonance in the antiferromagnetic heavy-fermion system UCu_5: spin reorientation at 1 K

H Nakamura†, Y Kitaoka‡, K Asayama‡, Y Ōnuki§ and M Shiga†

† Department of Materials Science and Engineering, Kyoto University, Kyoto 606-01, Japan
‡ Department of Material Physics, Osaka University, Toyonaka, Osaka 560, Japan
§ Department of Physics, Osaka University, Toyonaka, Osaka 560, Japan

Received 21 June 1994, in final form 15 August 1994

Abstract. The magnetic properties of UCu_5 with the C15b-type cubic crystal structure, which shows an antiferromagnetic transition at 15 K and, further, an unidentified transition at 1 K, were investigated by using the nuclear magnetic resonance (NMR) and nuclear quadrupole resonance (NQR) techniques. The measurements were performed for both crystallographically inequivalent Cu sites with cubic and trigonal symmetry in all the paramagnetic, antiferromagnetic and unidentified states. The results clearly indicate that the low-temperature state below 1 K is another antiferromagnetic state with a different spin structure from the high-temperature state. From the temperature variation of the field-swept spectrum, we propose a non-collinear quadruple-q (4-q) structure for the state between 15 and 1 K, which is different from the structure previously proposed by Murasik *et al* based on their neutron diffraction result. Furthermore, we propose a collinear single-q (1-q) structure for the state below 1 K, which cannot be distinguished from the 4-q structure by neutron diffraction. Assuming a simple model for hyperfine interactions and the magnetic structures, we consistently explain the complicated zero-field spectra obtained both above and below 1 K. The analysis shows clearly the spin reorientation at 1 K and that the variation of the local field at Cu sites is reasonably interpreted in terms of only the spin reorientation. The analysis also indicates that the electric field gradient changes significantly at 1 K, which is in contrast to no change at 15 K. The relation between the spin reorientation and the gap formation at 1 K is discussed.

1. Introduction

Electron correlation is one of the most attractive topics in condensed matter physics. Strongly correlated electrons exhibit a wide variety of exotic phenomena, which are not described by the conventional one-electron picture and remain to be interpreted by new concepts. A group of f-electron compounds called the heavy fermion (HF) system is a typical example, in which strongly correlated electrons play the leading part. The mass of electrons is enhanced from that of free electrons by the order of 10^2–10^3. The HF system usually shows the dense Kondo effect characterized by periodic local moments of f electrons at high temperatures. The correlated electrons form the coherent Kondo state at low temperatures, and the Kondo interaction competes with the Ruderman–Kittel–Kasuya–Yosida (RKKY) interaction, which favours alignment of magnetic moments. Generally, the HF state is formed as a result of suppression of magnetic ordering. Therefore, the typical examples of the ground state are superconducting, non-magnetic and weak antiferromagnetic states, although, in any cases, exotic types of magnetic correlation have been suggested by many experiments. For the systems with these ground states, the large γ value seems plausible because the slow reduction of entropy at low temperature causes a large specific heat.

0953-8984/94/4810567+26$19.50

A different type of HF state is seen in UCu_5, which exhibits an antiferromagnetic transition at 15 K. The specific heat shows a distinct enhancement of the temperature-linear coefficient, γ, above 1 K, suggesting the formation of an HF state in the antiferromagnetically ordered state (Ott *et al* 1985). Since UCu_5 already has a large ordered moment of the order of $1\mu_B$, it is mysterious that electrons behave as heavy quasiparticles. This suggests that a different type of degree of freedom should be taken into account. The large entropy leads to another phase transition at a very low temperature, i.e. in the vicinity of 1 K. Many experiments suggest that the transition appears to open gaps in the excitation spectrum of the heavy quasiparticles. However, the origin of this transition is still an open question. Thus, the HF state in antiferromagnetic UCu_5 is realized in a different situation from the conventional HF materials, which have non-magnetic or weakly magnetic state. Therefore, the unique nature of UCu_5 adds another variation to the HF systems and may give a hint for progress in the physics of strongly correlated electron systems. Especially, the origin of the transition at 1 K and the mechanism of gap formation should be important topics to be elucidated.

Here, we review briefly the experimental results of UCu_5. The antiferromagnetic transition at 15 K has been well known from the earlier stage and the antiferromagnetic state has been recognized as the ground state. Recently, however, Ott *et al* (1985) measured the low-temperature specific heat down to 0.15 K and discovered another phase transition in the vicinity of 1 K. The phase transition attracts much attention because the nature is quite anomalous and the origin of the transition is beyond our conventional knowledge. Furthermore, the result of the specific heat shows that the γ value is very large (380 mJ mol^{-1} K^{-2}) just above 1 K, indicating the presence of heavy electrons in the magnetically ordered state. The magnetic susceptibility shows a Curie–Weiss-like behaviour (Misiuk *et al* 1973, Brodsky and Bridger 1973, van Daal *et al* 1975, Coldea *et al* 1976, Coldea and Pop 1985, Zolnierek *et al* 1987, Ōnuki *et al* 1989a, Takagi *et al* 1989). Various values of the effective moment P_{eff} and the paramagnetic Curie temperature θ_p, which scatter largely from 2.3 to $3.6\mu_B$ and from -78 to -260 K, respectively, were reported by those authors. The determination of 5f-electron configuration is important especially for the localized moment scheme. Because of large scattering of experimental P_{eff}, it is very difficult to determine the valence of U atoms even at high temperature from the magnetic data. Actually there is no reliable discussion on the crystal-field ground state of the U atom in UCu_5. The large scattering of experimental results seems to indicate that P_{eff} and θ_p are rather temperature-dependent, which suggests that 5f electrons are in the mixed-valent state and that the degree of localization is dependent on temperature. A mixed-valent state of U was first suggested by van Daal *et al* (1975), who claimed a mixed-valence configuration between $5f^2$ and $5f^3$. Grohs *et al* (1980) supported the idea by the result of x-ray photoemission spectroscopy (XPS). Walter *et al* (1987) measured inelastic neutron scattering and observed a broad Lorentzian quasielastic line with a width of the order of $\Gamma \sim 10$ meV, which is higher by one order than that of T_N. This suggests that 5f electrons interact strongly with conduction electrons or with other magnetic moments. Takagi *et al* (1989) also pointed out the strong hybridization between 5f and conduction electrons from their Cu nuclear magnetic relaxation measurement. The electrical resistivity exhibits, in the paramagnetic state, a Kondo-like increase with decreasing temperature as usually seen for the HF systems (Brodsky and Bridger 1973, van Daal *et al* 1975, Ott *et al* 1985, Ōnuki *et al* 1989a,b). From these results, UCu_5 is considered, at present, as one of the typical dense Kondo substances with a strong interaction between 5f and conduction electrons.

As for the antiferromagnetic transition at 15 K, the nature is, in some sense, conventional. At around T_N, the magnetic susceptibility has a broad hump as usually seen for classical

antiferromagnets. Specific heat has a λ-type peak (van Daal *et al* 1975, Ott *et al* 1985). Microscopic measurements such as neutron diffraction (Murasik *et al* 1974) and muon spin relaxation (μSR) (Barth *et al* 1986) also show a conventional behaviour. On the other hand, several unconventional features were also reported. For example, the entropy developed in the magnetic transition has a low value of $0.59R\ln 2$ (van Daal *et al* 1975), which is much smaller than that of a free U ion, $R\ln 6$ to $R\ln 10$. With decreasing temperature, the electrical resistivity increases sharply around T_N deviating from the Kondo-like behaviour, has a maximum around 10 K and decreases rapidly down to 1 K. It was pointed out that the feature is similar to that of Cr, which undergoes a transition to the spin-density-wave (SDW) state. The magnetic structure was determined by neutron diffraction measurement. Murasik *et al* (1974) measured a polycrystalline sample and proposed a simple antiferromagnetic structure of collinear type, which will be discussed in detail in section 2. The result was again evidenced by another neutron diffraction study by Chakravarthy *et al* (1985). The magnetic moments per U atom were estimated to be 0.9 ± 0.1 and $1.3 \pm 0.2\mu_B$ by the former and latter authors, respectively. Further, Schenck *et al* (1990) recently reported a larger value, $1.55 \pm 0.05\mu_B$.

The exotic transition at 1 K has been evidenced by various measurements. The specific heat measured by Ott *et al* (1985) shows a large peak around 1 K accompanied by thermal hysteresis with $\Delta T = 0.17$ K, indicating that the transition is of first order. The electrical resistivity increases by a factor of 7 with decreasing temperature, and seems to saturate to a fairly large value at the lowest temperature in contrast to very small values for other typical HF compounds (Ott *et al* 1985). A similar behaviour was also observed for the Hall coefficient, indicating a marked reduction of carriers at the transition (Ōnuki *et al* 1989a, b). These anomalies are interpreted as an energy-gap formation in the excitation spectrum of the heavy quasiparticles.

Nuclear magnetic resonance (NMR) and nuclear quadrupole resonance (NQR) are useful microscopic methods to study magnetic materials. They give selected information on locally different atomic sites. One can get information on the magnetic structure by discussing the amplitude and direction of the local field at nuclear sites. Hence, the NMR and NQR experiments are very useful to study HF materials especially at low temperatures. In the present study of UCu_5, we have measured ^{63,65}Cu NMR and NQR in all the paramagnetic, antiferromagnetic and unidentified states in order to determine the magnetic structure below T_N, to clarify the state below 1 K and to investigate the nature of the transition at 1 K. From the analysis of the NMR spectra, we propose a new type of structure for the antiferromagnetic state between 15 and 1 K, which explains both the NMR and neutron diffraction data consistently. It will be clarified that the state below 1 K is another antiferromagnetic state with a different spin structure. The origin of the transition at 1 K accompanied by spin reorientation is also discussed. From the experimental point of view, we emphasize that the NMR of the crystallographically different Cu sites in different local symmetry gives quite useful information to determine the spin orientation in the ordered state. Parts of the study have already been published as conference papers (Nakamura *et al* 1990, 1991).

2. Possible magnetic structures of UCu_5

2.1. Results of neutron diffraction

Most simply, if the magnetic arrangement in a crystalline lattice has a period of a/q, where a is the lattice constant, the magnetic moment at a position r can be expressed as

$$m(r) = m_0 \exp(2\pi i q \cdot r) \tag{1}$$

where m_0 is the amplitude and direction of magnetic moment, In this case, the elastic magnetic scattering cross section of neutron diffraction at a given scattering vector $K = \tau + q$, where τ is the reciprocal lattice vector, is given by

$$d\sigma/d\Omega = Cf^2 m_0^2 \sin^2\alpha \tag{2}$$

where C is a constant depending on the crystal, f is the magnetic form factor of the magnetic ions and α is the angle between the scattering vector and the direction of magnetic moments.

UCu_5 crystallizes in the cubic $AuBe_5$-type structure with lattice constant $a = 7.04$ Å (Baenziger *et al* 1950), in which uranium atoms form the face-centred cubic (FCC) lattice. (Details will be discussed in section 3.) The Brillouin zone of the FCC lattice has four high-symmetry points, $\Gamma(0, 0, 0)$, $X(0, 0, 1)$, $L(\frac{1}{2}, \frac{1}{2}, \frac{1}{2})$ and $W(1, \frac{1}{2}, 0)$. If the q vector is at the X point, the antiferromagnetic structure is called type I, at the L point type II and at the W point type III. Neutron diffraction experiment (Murasik *et al* 1974) revealed that the magnetic structure of UCu_5 is of the type-II antiferromagnet characterized by $q = (\frac{1}{2}, \frac{1}{2}, \frac{1}{2})$. Another important result of neutron diffraction is the absence of magnetic (111) peak in the magnetically ordered state. Generally, the reflection from (111) planes does not vanish for the type-II antiferromagnets. From equation (2), the (111) reflection disappears in the case $\sin\alpha = 0$. Hence, the authors concluded that the magnetic moment is parallel to ⟨111⟩ axis. From these results they proposed a simple antiferromagnetic structure, as shown in figure 1(*a*), which consists of parallel (111) planes in which U moments order ferromagnetically but couple antiferromagnetically between neighbouring sheets. As will be mentioned below, however, this structure is inconsistent with the results of NMR at 1.4 K. Therefore, a more general treatment is necessary to discuss the magnetic structure of UCu_5.

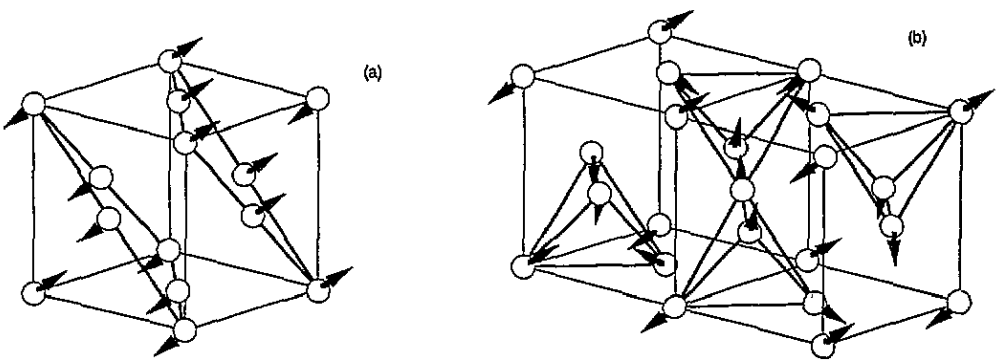

Figure 1. Possible antiferromagnetic structures of UCu_5 with assumptions that (i) each Fourier component of magnetic moment is parallel to the corresponding modulation vector, and (ii) each magnetic ion has the same magnetic moment value: (*a*) and (*b*) are 1-*q* and 4-*q* structures, respectively.

Recently, Schenck *et al* (1990) measured neutron diffraction at both 10 mK and 1.34 K and found that the intensity of the magnetic scattering does not change, within an accuracy of ±5%. They concluded that neither crystal structural nor magnetic structural transition takes place at 1 K and interpreted the transition at 1 K in terms of some additional small-moment magnetic ordering or the SDW phenomenon.

2.2. *Possible structures*

Here, we extend the possible candidates of the magnetic structure to multiple-q structures. Generally, a long-range ordering of magnetic moments is expressed by a Fourier expansion of q,

$$m(r) = \sum_i m_i \exp(2\pi i q_i \cdot r) \tag{3}$$

where q_i means a set of vectors belonging to the star of q and restricted to the first Brillouin zone. The summation is taken over all q_i components. The star of $q = (\frac{1}{2}, \frac{1}{2}, \frac{1}{2})$ characterizing the type-II antiferromagnetic structure, i.e. $\{\frac{1}{2}, \frac{1}{2}, \frac{1}{2}\}$, has four vectors,

$$q_1 = (\tfrac{1}{2}, \tfrac{1}{2}, \tfrac{1}{2}) \qquad q_2 = (-\tfrac{1}{2}, \tfrac{1}{2}, \tfrac{1}{2}) \qquad q_3 = (\tfrac{1}{2}, -\tfrac{1}{2}, \tfrac{1}{2}) \qquad q_4 = (\tfrac{1}{2}, \tfrac{1}{2}, -\tfrac{1}{2}). \tag{4}$$

In some conditions, the multiple-q structure can be formed as a linear combination of some of the four symmetric states. They are, in general, non-collinear structures. For the type-II antiferromagnets, 1-, 2-, 3- and 4-q states should be taken into account depending on the number of superpositions of different q_i terms. Experimentally, it is difficult to distinguish the multiple-q structure from the 1-q structure with a multi-domain configuration. Especially, if the multiple-q structure can be denoted as a linear combination of several 1-q states with a volume v_i, neutron diffraction experiment gives an identical Bragg diffraction pattern with the 1-q system in which each domain has a volume v_i. Thus, the magnetic structure of UCu_5 should be examined more generally by taking into account the possible multiple-q structures.

The multiple-q structures were first discussed for 3d transition-metal oxides and alloys and, afterwards, also investigated extensively for the intermetallic compounds containing a rare earth or uranium (see, for example, Rossat-Mignod 1987). The intensity of magnetic diffraction for multiple-q structures was calculated by several authors (Roth 1958, van Laar 1965). The multiple-q structures for the type-II antiferromagnets were first discussed by Roth (1958) in connection with the magnetic structures of transition-metal monoxides. Afterwards, Herrmann-Ronzaud *et al* (1978) investigated the possible equivalent multiple-q structures of the type-II antiferromagnets in terms of the group-theoretical analysis based on symmetry considerations and imposing a physical restriction. They enumerated several structures as possible structures. Here, we consider the possible magnetic structures of UCu_5 following their discussion.

In order to simplify the discussion, we refer to the results of neutron diffraction. In the magnetically ordered state, the (111) scattering peak was not observed. For the type-II antiferromagnets, the condition is attained only when each Fourier component m_i is parallel or antiparallel to corresponding q_i even in the multiple-q states as well as in the 1-q state. Therefore, we impose the following two conditions to restrict the number of possible magnetic structures of UCu_5.

(i) The magnetic moment distribution can be written by equation (3) where q_i takes some of the four vectors defined in equation (4), and each Fourier component m_i is parallel to the corresponding q_i. In this case, the vector m_i can be described by only z-axis scalar component m_i by taking the z axis along the $\langle 111 \rangle$ direction.

(ii) Each magnetic ion has the same magnetic moment value, i.e.

$$m(r)^2 = m_0^2. \tag{5}$$

This can be rewritten with the possible set of coefficients, m_i, as

$$\sum_{i=1}^{4} m_i^2 = m_0^2. \tag{6}$$

In this case, the second assumption markedly reduces the possible combinations of m_i, as was pointed out by Herrmann-Ronzaud *et al* (1978). It is easily found that only one 1-q structure and one 4-q structure satisfy equation (6). Those structures are shown in figures 1(a) and (b). The 1-q structure (figure 1(a)) is the spin arrangement proposed by Murasik *et al* (1974) for UCu_5. The 4-q structure shown in figure 1(b) is a part of the unit cell, which is given by equation (3) using all vector q_i in equation (4) and taking appropriate m_i. The 4-q structure was first proposed by Roth (1958) and discussed in detail by Herrmann-Ronzaud *et al* (1978). It should be noted that the 4-q structure has cubic symmetry ($m3m$) in contrast to the trigonal symmetry ($\bar{3}m$) of the 1-q system. In the 4-q structure, the moments are directed to or from the centre of the tetrahedron along each of the general $\langle 111 \rangle$ axes. It should be noted that if each q domain in the 1-q state has a volume $v_i = V/4$, where V is the total volume, these two structures are equivalent from the standpoint of neutron diffraction. In principle, it is possible to distinguish these structures by changing the volume fraction of domains, i.e. by applying some external perturbation such as magnetic field and pressure. It is, however, very hard to detect a significant difference in those experiments.

3. Experimental procedures

UCu_5 is only one intermetallic compound in the U–Cu binary system. Because of the formation by the peritectic reaction, a single phase is hard to obtain. In the present study, we used polycrystalline samples prepared by arc-melting. A little off-stoichiometric amount of U and $Cu_{4.95}$ was melted so as to avoid precipitation of Cu, and annealed at 800 °C for a week. For NMR measurement the ingot was crushed into fine powder with particle diameter smaller than 50 μm. Empirically, the powder of UCu_5 is very unstable because it is easily oxidized. As a result of oxidation of U, redundant metallic Cu precipitates preferentially on the surface of particles. Therefore, the powder was sealed in helium atmosphere, and the measurement was carried out within several days after crushing in order to avoid unnecessary oxidation and the precipitation of impurity phases.

Spin-echo measurement was carried out by a conventional phase-coherent pulsed spectrometer. The low temperature below 1 K was obtained by a conventional ^{3}He refrigerator. As the gyromagnetic ratios of ^{63}Cu and ^{65}Cu, the values $^{63}\gamma/2\pi$ = 1.1285 MHz kOe^{-1} and $^{65}\gamma/2\pi$ = 1.2089 MHz kOe^{-1} were used.

For the convenience of NMR experiments, crystallographic information on UCu_5 is reviewed. UCu_5 forms cubic C15b-type structure (space group $F\bar{4}3m$, $[T_d^2]$), which is also called $AuBe_5$-type structure. The sketch of the unit cell is shown in figure 2(a). In this structure, Cu atoms are surrounded by an FCC network (4a site) of U atoms and have two crystallographically inequivalent Cu sites characterized by large (4c site) and small (16e site) tetrahedra (see figures 2(b) and (c)). In some literature, the former and latter Cu sites were denoted as sites I and II, respectively. Here, we will call these sites *4c site* and *16e site*. This structure type is closely related to the cubic Laves-phase structure (C15), in which the 4c site is occupied by the minority atoms, leading to a composition 1:2 rather

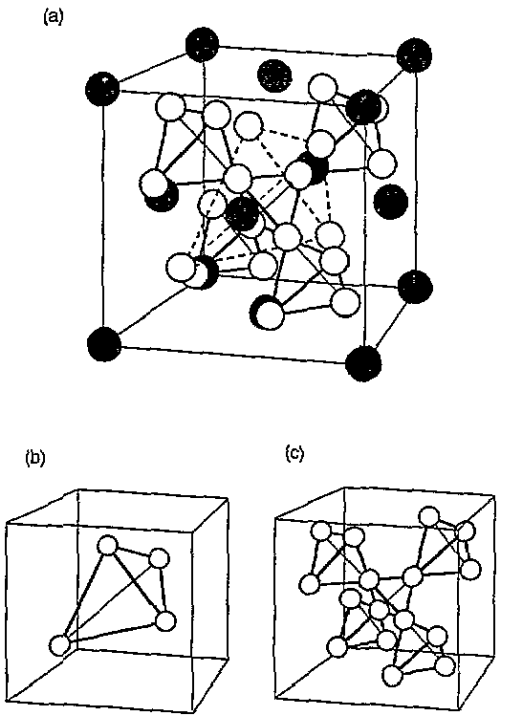

Figure 2. (*a*) Crystal structure of UCu_5 (C15b-type): full and open circles represent U and Cu atoms, respectively. (*b*), (*c*) Crystallographic Cu sites in UCu_5: the 4c site with cubic symmetry (*b*) and the 16e site with trigonal symmetry (*c*).

than 1:5. The positions of the Cu atoms are described by the following coordinates with the face-centring translation $(0, 0, 0)+$, $(0, \frac{1}{2}, \frac{1}{2})+$, $(\frac{1}{2}, 0, \frac{1}{2})+$ and $(\frac{1}{2}, \frac{1}{2}, 0)+$:

$$\begin{array}{ll} \text{4c site} & (\tfrac{1}{4}, \tfrac{1}{4}, \tfrac{1}{4}) \\ \text{16e site} & (x, x, x), (x, -x, -x), (-x, x, -x), (-x, -x, x). \end{array} \tag{7}$$

For the perfect closed-packed arrangement, $x = 5/8 = 0.625$. Murasik *et al* (1974) reported that the neutron diffraction intensities were in good agreement with calculated intensities with $x = 0.626$. This indicates that Cu atoms of the 16e site occupy substantially ideal positions. It should be noted that the 4c site has cubic symmetry ($\bar{4}3m$) while the 16e site has trigonal one ($3m$) around one of the $\langle 111 \rangle$ axes. Thus, the 16e site feels a finite electric field gradient (EFG), $eq = V_{zz}$, with the anisotropy parameter $\eta = (V_{xx} - V_{yy})/V_{zz} = 0$, where V_{xx}, V_{yy} and V_{zz} are the diagonal components of the EFG tensor at the nucleus. The nearest-neighbour (NN) and the next-nearest-neighbour (NNN) atoms of the 4c site are twelve Cu atoms at the 16e site and four U atoms, respectively. The NN atoms of the 16e sites are six Cu atoms at the 16e site and their NNN atoms are three U atoms and three Cu atoms at the 4c site.

4. Experimental results

4.1. Paramagnetic state

4.1.1. NMR spectrum. Figure 3 shows the field-swept NMR spectrum of ^{63}Cu in UCu_5 at 125.1 MHz and 120 K. A powder pattern characterized by the first-order electric quadrupolar interaction is seen in figure 3(*a*). Since only the 16e site feels a finite EFG as mentioned above, the resonance is assigned to the 16e site. The NQR of this site was also observed, as will be shown below. The magnification of the central part is shown in figure 3(*b*). This pattern consists of three different components. One is the second-order quadupolar powder pattern of the 16e site with a small anisotropy effect. Singularity edges corresponding to $\theta = 0°$ and $\theta = \zeta$ are clearly resolved, where θ means the angle between the external field and the local symmetry axis of the Cu site and ζ becomes $\sim 41.8°$ in the case with no anisotropy effect. Although the structure is slightly smeared by an inhomogeneous broadening, a step corresponding to $\theta = 90°$ is also observable around 11.10–11.11 T. Another is a very sharp line observed at a field with almost zero Knight shift K, which is assigned to the 4c site with cubic symmetry. In experiments at low frequencies, only this sharp line was observable because the signal from the 16e site disappears provided that the Zeeman interaction is smaller than the quadrupolar interaction. The other is the signal seen at the lower-field side of the sharpest resonance. This is an extrinsic signal, which is probably assigned to the impurity Cu in pure metallic state, because the reonance field and the nuclear spin–lattice relaxation time T_1 just correspond to those of metallic Cu. Empirically, the intensity of this signal depends sensitively on the sample quality. The intensity becomes larger with time after crushing of the sample ingot. This may be ascribed to the oxidation of U on the grain surface, which causes the precipitation of metallic Cu. In the NMR measurements of UCu_5, an impurity signal is frequently observed in spite of careful treatment of the sample. Buschow *et al* (1979) also reported that the signal of Cu metal was observed in their NMR measurement. Since the identification of the Cu signal with $K \sim 0$ has critical significance in the discussion of magnetic structure, the greatest attention was paid to the origin through our whole measurements.

From the local symmetry of the 16e site, both the Knight-shift tensor and the EFG tensor are uniaxial, having the same principal axis along the ⟨111⟩ axis. For the nuclear spin $I = 3/2$ in axial symmetry, the resonance frequency of the $m \leftrightarrow (m-1)$ transition is given within the second-order perturbation theory by

$$\nu_m = \nu_0 + [\tfrac{1}{2}\nu_Q(m-\tfrac{1}{2}) + K_{ax}\nu_R](3\cos^2\theta - 1) - (\nu_Q^2/16\nu_0)(\cos^2\theta - 1) \times \{[204m(m-1) - 57]\cos^2\theta - 12m(m-1) + 9\} \quad (8)$$

where K_{ax} is the axial Knight shift, ν_0 is the true centre of the resonance and ν_R is the resonance frequency of a reference material (see, for example, Carter *et al* 1977 p 64). The pure quadrupole frequency ν_Q is written for the nuclear spin $I = 3/2$ in uniaxial local symmetry as

$$\nu_Q = \tfrac{1}{2}e^2qQ/h \quad (9)$$

where Q is the quadrupole moment of the nucleus. From equation (8), we have $\nu_{3/2} - \nu_{-1/2} = \nu_Q$. This indicates that, although the first-order satellites are shifted by the anisotropy effect, the separation between the satellite pairs is not affected within the second-order perturbation, and gives the value of ν_Q. The analysis of first-order satellite pairs at 120 K gives a value, $^{63}\nu_Q = 12.74 \pm 0.05$ MHz, which will be compared with the value given by NQR measurement.

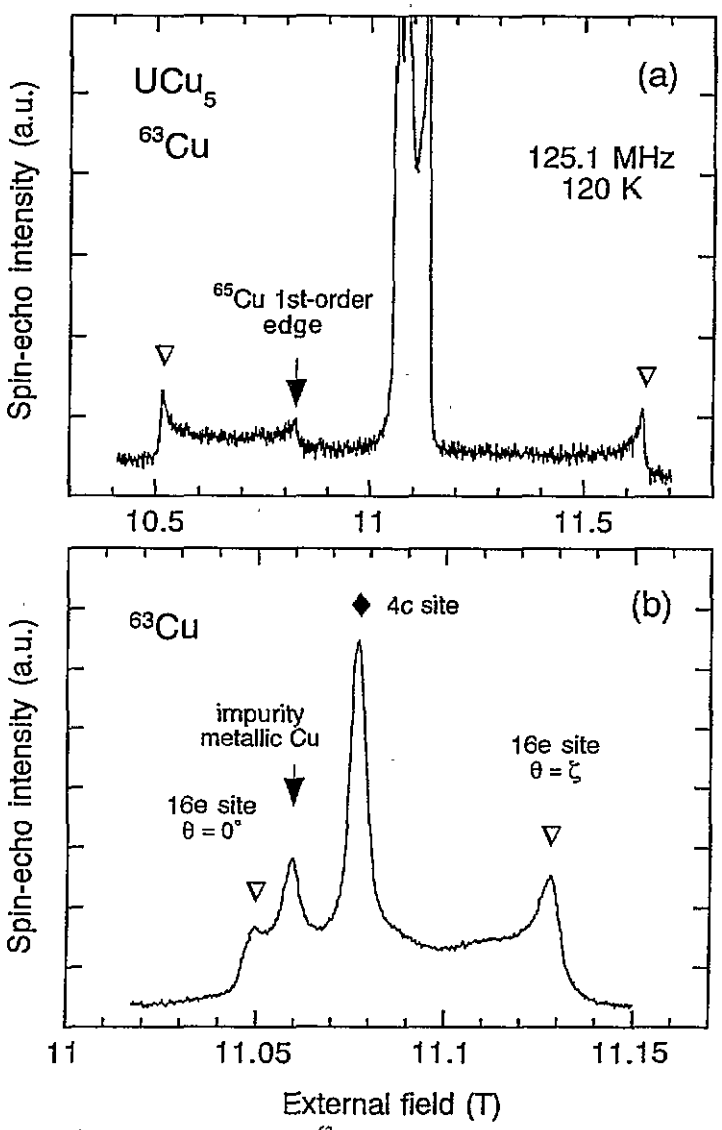

Figure 3. Field-swept spectrum of ^{63}Cu in UCu_5 at 125.1 MHz and 120 K. (*a*) Singular edges of the first-order quadrupolar powder pattern of 16e site are indicated by open triangles. (*b*) Magnification of the central resonance. Open triangles indicate the second-order singular edges of 16e site; full diamond indicates the resonance from 4c site. For details see text.

4.1.2. NQR spectrum. In the paramagnetic state, we also observed the Cu NQR signal in zero applied field. Figure 4 shows the ^{63}Cu and ^{65}Cu NQR spectrum at 30 K. These signals correspond to $m = \pm 3/2 \leftrightarrow m = \pm 1/2$ transitions caused by the electric quadrupolar interaction and are assigned to the 16e site. From the centre of gravity of the line, ν_Q at 30 K is estimated to be 12.824 MHz for ^{63}Cu. This agrees well with those obtained by Buschow *et al* (1979) and Takagi *et al* (1989). The spectrum is fitted well with a Gaussian function with full width at half-maximum of 74 kHz.

We measured the temperature dependence of ν_Q of ^{63}Cu by following the NQR spectrum

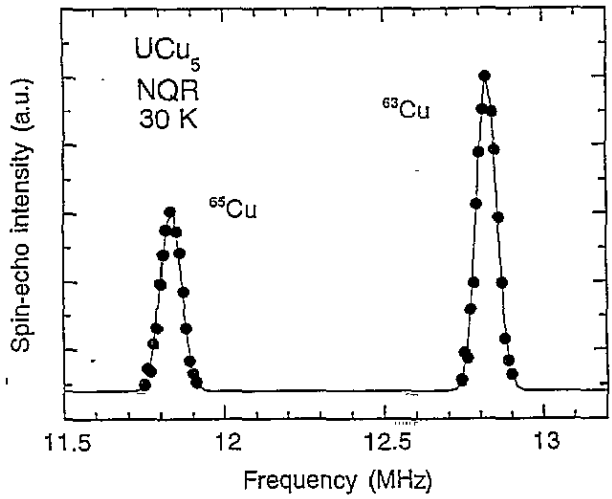

Figure 4. Cu NQR spectrum of UCu_5 at 30 K.

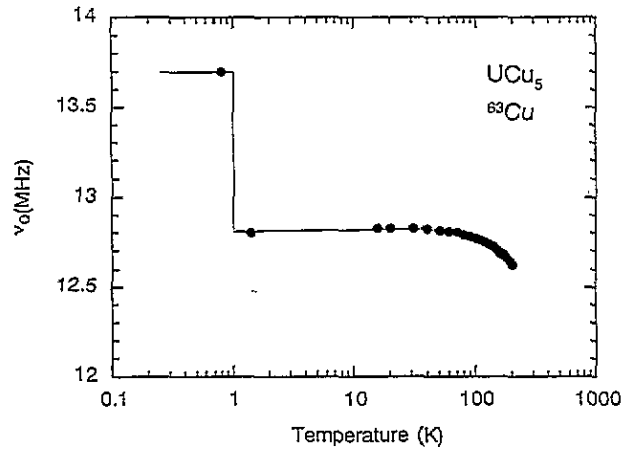

Figure 5. Temperature dependence of ν_Q of ^{63}Cu in UCu_5 measured by the NQR experiment in the paramagnetic state and estimated from the analysis of zero-field spectra in the magnetically ordered state. The full curve is a guide for the eye.

up to 200 K. The result is shown in figure 5. The quadrupole frequency decreases gradually with increasing temperature. The origin of the temperature dependence will be discussed in section 5.3. For a comparison, we list ν_Q of ^{63}Cu at 120 K, namely $^{63}\nu_Q = 12.748 \pm 0.010$ MHz. This is in good agreement with that estimated from the field-swept spectrum. This indicates that the field dependence of ν_Q is negligible.

4.2. Antiferromagnetic state between 15 and 1 K

4.2.1. Field-swept spectrum. Figure 6 shows the field-swept spectrum of ^{63}Cu in the antiferromagnetic state (4.2 K). The first-order quadrupolar pattern of the 16e site is smeared, being associated with the onset of antiferromagnetism. On the other hand, the sharp central peak with $K \sim 0$ remains even in the antiferromagnetic state. This seems to indicate that the internal field is cancelled at certain Cu sites. However, we should take care over the origin of the resonance because paramagnetic impurity phases containing Cu may lead to a

resonance with $K \sim 0$. Actually, another signal that is ascribed to Cu metal was observed just near the central resonance. Therefore, it is very important to discriminate the intrinsic signal from the impurity one. In order to emphasize the origin of the Cu NMR signal, we performed several experiments.

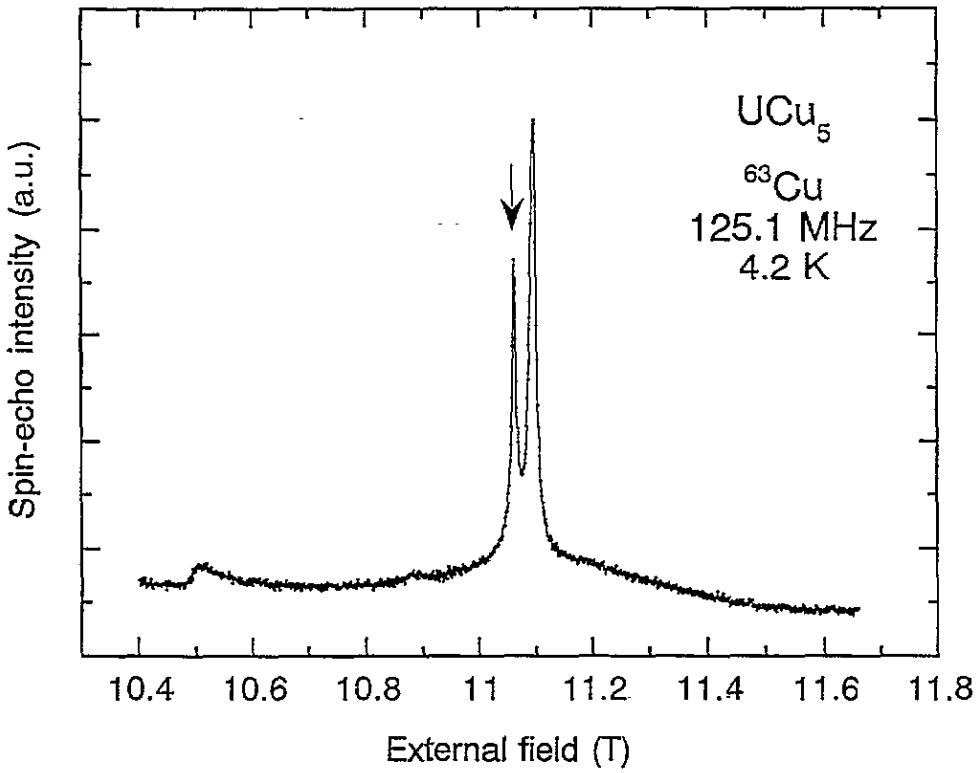

Figure 6. ^{63}Cu field-swept spectrum of UCu_5 at 4.2 K measured at 125.1 MHz. The signal marked by the arrow is an extrinsic resonance of impurity metallic Cu.

Figure 7 shows the temperature dependence of the resonance field of the central line measured at a frequency of 125.1 MHz. The resonance field changes discontinuously just below T_N. This indicates that, although the resonance does not feel a large internal field even in the antiferromagnetic state, it is clearly correlated with the antiferromagnetic transition. On the other hand, the resonance field of impurity Cu is not influenced by the transition at all. It should be noted that the resonance shift becomes negative below T_N. (The zero-shift field of ^{63}Cu at 125.1 MHz is 11.0855 T.) We also measured a sample with worse quality at a relatively low frequency and at 4.2 K. The result was reported in a previous paper (Nakamura *et al* 1991). In a certain pulse condition, two different signals were observed. One is the resonance with $K \sim 0$ and the other is that with the Knight shift of pure Cu. We measured T_1 of the latter signal and confirmed that the value just coincides with that of pure Cu. On the other hand, T_1 of the signal with $K \sim 0$ is clearly related to the transition at 15 K, i.e. $1/T_1$ rapidly increases up to 15 K with increasing temperature, and the signal disappears suddenly below 1 K as will be described in the next section. From these results, we conclude that the signal with $K \sim 0$ is the intrinisic resonance of UCu_5. It

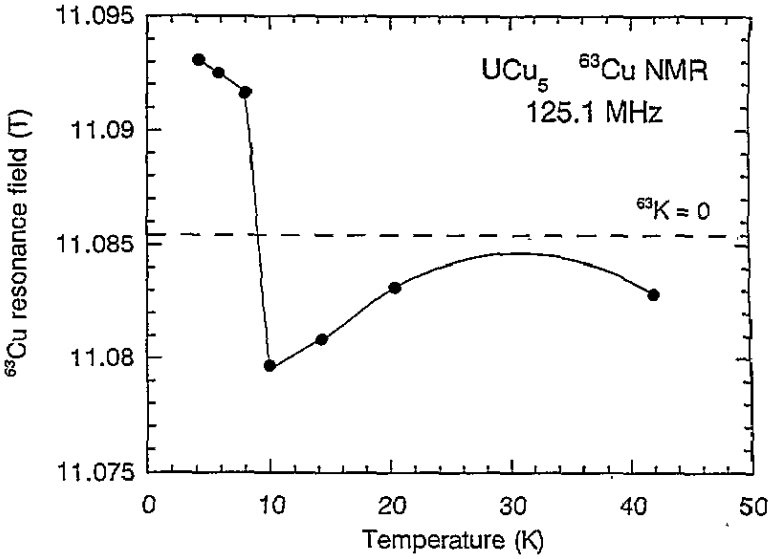

Figure 7. Temperature dependence of resonance field of ^{63}Cu signal with almost zero Knight shift for UCu_5 measured at a frequency of 125.1 MHz. The broken line indicates the field with zero Knight shift for ^{63}Cu.

is also notable that the spin-echo decay time of the extrinsic signal is comparatively short. The intrinsic signal can be separated by making use of the large difference of spin-echo decay time between these two signals. The presence of the intrinsic signal with $K \sim 0$ apparently indicates that a part (or all) of the 4c site feels almost no internal field even in the magnetically ordered state.

4.2.2. Zero-field spectrum. Below T_N, the NQR spectrum is markedly modified by the onset of the static local field induced by the ordering of U moments. The zero-field spectrum at 1.4 K is shown in figure 8(*a*), where several peaks are seen in the frequency range between 5 and 22 MHz. The spectrum has a very complicated structure because the magnitude of the electric quadrupole interaction of the 16e site is comparable to the Zeeman interaction with the internal field produced by U moments. As will be discussed in section 5.2, the signals marked by the arrows in the figure are assigned to the resonance from ^{63}Cu and ^{65}Cu at the 4c site with cubic symmetry. Taking into account the result of the field-sweep experiment, it is concluded that the 4c site is separated into different magnetic sites in the antiferromagnetic state and that one of them feels no local field and the other feels a finite field. (We will denote the former and latter sites as 4c-I and 4c-II sites, respectively, in section 5.1.2.) Since the 4c site has cubic local symmetry the resonance field just corresponds to the magnitude of the hyperfine field at the site. We measured the temperature dependence of ^{63}Cu resonance frequency of the 4c-II site below 13 K. The estimated temperature dependence of the hyperfine field at the 4c-II site is shown in figure 9. With temperature approaching T_N, the hyperfine field decreases, as usually seen for a second-order magnetic phase transition. Above 13 K, the signal intensity is too small to be detected.

4.3. Unidentified state below 1 K

4.3.1. Field-swept spectrum. Figure 10 shows field-swept NMR spectra of ^{63}Cu measured at a low frequency of 6.97 MHz and at 1.43 and 0.69 K. As shown above, the signal with

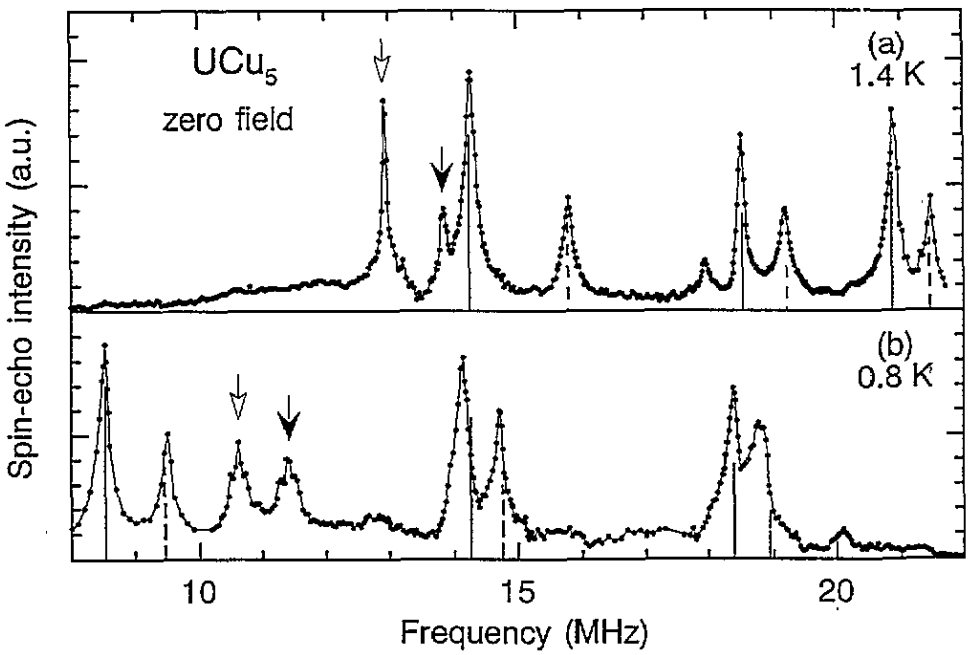

Figure 8. Cu zero-field spectra of UCu_5 at (*a*) 1.4 K and (*b*) 0.8 K. Open and full arrows indicate ^{63}Cu and ^{65}Cu signals from the 4c-II site, respectively. Full and broken vertical lines represent best-fit calculated frequencies of ^{63}Cu and ^{65}Cu resonances, respectively, which are assigned to the 16e-II site. The height of the lines indicates, only for reference, the calculated transition probability.

$K \sim 0$ was observed at 1.43 K. In this experimental condition with a relatively short repeat time of 100 ms, only the intrinsic signal was observed. With decreasing temperature, this signal suddenly disappears at 1 K and no resonance was observed below 1 K. The spectrum at 0.69 K shown in figure 10 was measured with a relatively long repeat time of 3 s. In this condition, a different signal appears at the metallic Knight shift of Cu. As discussed above, this may be ascribed to the Cu metal involved as an impurity phase. In order to identify unequivocally the origin of this signal in this temperature range, we carefully measured the temperature dependence of T_1 and the Knight shift between 0.4 and 1 K. The shift is independent of temperature and T_1 obeys the Korringa law with the relaxation rate of pure Cu. Therefore, it is concluded that the intrinsic NMR signal with $K \sim 0$ disappears below 1 K.

4.3.2. Zero-field spectrum. At around 1 K, the zero-field spectrum is also discontinuously modified corresponding to the first-order phase transition. Figure 8(*b*) shows the spectrum at 0.8 K. We observed several peaks in almost the same frequency range of the spectrum above 1 K. In the spectrum, several pairs of resonance lines corresponding to ^{63}Cu and ^{65}Cu are seen. The ratio of the signal intensities of the pair should be that of the abundances of ^{63}Cu and ^{65}Cu atoms. However, the result does not satisfy this relation. This is reasonably explained as follows. The measurement was performed using repeating times of the order of 1 s. This is not long enough for the nuclear magnetization to recover completely owing to the long T_1 (Nakamura *et al* in preparation). In this condition, the intensity of ^{63}Cu is

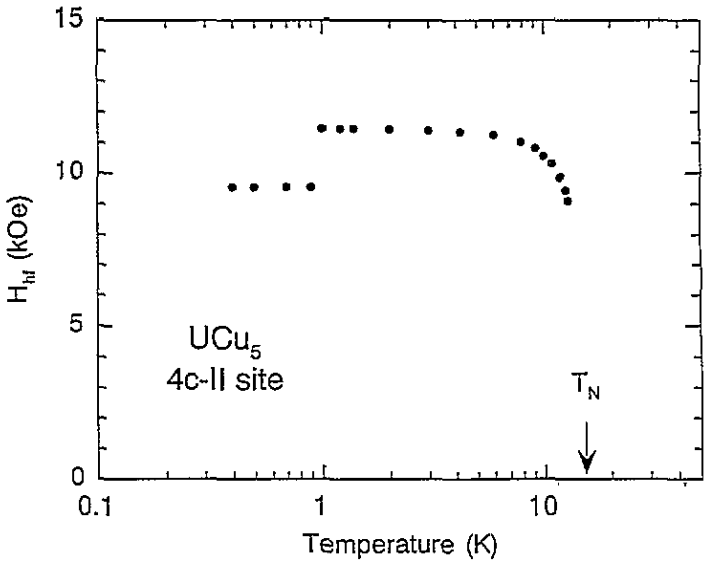

Figure 9. Temperature dependence of the hyperfine field at the 4c-II site in UCu_5 between 0.4 and 13 K.

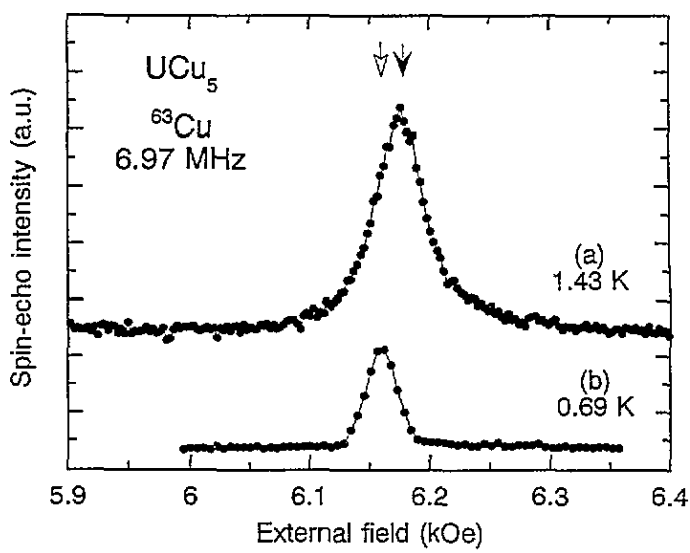

Figure 10. ^{63}Cu NMR spectra of UCu_5 at (*a*) 1.43 and (*b*) 0.69 K measured at 6.97 MHz. Full and open arrows indicate the position of zero Knight shift and metallic Knight shift of ^{63}Cu, respectively. The repeat time is 100 ms and 3 s for (*a*) and (*b*), respectively. In the condition of (*a*), the impurity signal is not observable because of its long T_1.

more reduced than ^{65}Cu because T_1, being proportional to γ^2 provided that the relaxation is dominated by the magnetic hyperfine mechanism, is longer for ^{63}Cu than for ^{65}Cu. Anyhow, this spectrum indicates unambigously the presence of the internal field. Since Schenck *et al* (1990) did not find any difference between neutron diffraction patterns at 1.34 K and 10 mK,

they claimed that there is neither a structural nor a magnetic phase transition near 1 K in a conventional sense. However, our NMR result undoubtedly demonstrates the occurrence of a first-order phase transition accompanied by a considerable variation of magnetic parameters. Most naturally, the reorientation of the ordered spins is suggested.

As will be discussed in section 5.2, only signals marked by arrows can be assigned to the 4c site, which will be denoted as the 4c-II site in section 5.1.2. The resonance frequency directly corresponds to the local field at the 4c-II site. The temperature dependence of the estimated field is shown in figure 9. The figure indicates clearly that the hyperfine field is constant below 1 K and jumps discontinuously at 1 K.

5. Analysis and discussion

5.1. Determination of magnetic structure

As will be mentioned below, the 1-q structure proposed by Murasik *et al* (1974) is inconsistent with our NMR results between 15 and 1 K. Therefore, we should examine more generally the possible magnetic structures. As already discussed in section 2, only two magnetic arrangements satisfy the neutron diffraction data of UCu_5 by applying two simple assumptions. To analyse NMR results, we confine our attention to these two candidates, i.e. the 1-q and 4-q structures shown in figure 1. First, we will describe our model for the hyperfine interaction of Cu nucleus with U moment; secondly, enumerate the expected magnetic sites of Cu assuming those two magnetic structures; and, last, determine the magnetic structures for both high-temperature and low-temperature states.

5.1.1. Model of local field at Cu sites. In the magnetically ordered state, the Cu NMR experiment gives information on the transferred field from U moments to Cu sites. In order to discuss the magnetic arrangement of the U lattice, we need knowledge of the hyperfine mechanism from U moments to Cu nuclei. Here, rather phenomenologically, we define the local field at Cu sites:

$$\boldsymbol{H}_{\mathrm{loc}} = \boldsymbol{H}_{\mathrm{iso}} + \boldsymbol{H}_{\mathrm{dip}}. \tag{10}$$

The first term is the transferred hyperfine field from near-neighbour U moments. By assuming that all the anisotropic contribution is negligibly small, we only consider the isotropic contribution. The second term is the anisotropic field, which is assumed to be only the lattice dipole field.

The anisotropic dipole field from U moments is calculated by a classical dipole sum,

$$\boldsymbol{H}_{\mathrm{dip}} = \sum_j \left(\frac{3(\boldsymbol{m}_j \cdot \boldsymbol{r}_j)\boldsymbol{r}_j}{r_j^5} - \frac{\boldsymbol{m}_j}{r_j^3} \right) \tag{11}$$

where $\boldsymbol{m}_j$ and $\boldsymbol{r}_j$ are the magnetic moment and position of the jth U site. The Cu nucleus is taken as the origin of the coordinate system.

On the other hand, it is very difficult to discuss quantitatively the isotropic transferred hyperfine mechanism. As isotropic interactions in UCu_5, the following mechanisms may be considered: (i) the polarization of conduction electrons caused by the exchange interactions with spin-polarized U 5f electrons (classical RKKY interaction); (ii) the polarization of s-like electrons of Cu caused by direct or indirect exchange interactions through the mixing with 5f electrons of neighbouring U atoms. Usually, for f-electron systems, the second

contribution is small because the f-electron wavefunction is restricted to the inner core due to the shielding of outer electrons. For UCu_5, it is easily accepted that the first contribution is one of the possible mechanisms of the transferred hyperfine interaction. Nevertheless, for UCu_5, crystal-field splitting was not detected, but a broad Lorentzian quasielastic spectrum with width of order $\Gamma \sim 10$ meV was observed by inelastic neutron scattering (Walter *et al* 1987). Therefore, although a Curie–Weiss-like behaviour of susceptibility was observed for UCu_5, it is likely that Kondo temperature T_K of UCu_5 is rather high and is of the order of 100 K. For such a case, direct mixing between U 5f and Cu wavefunctions may be important. Therefore, the second contribution may be dominant in UCu_5 especially at low temperatures. In any case, the hyperfine field at Cu sites is produced via the polarization of s-like electrons of Cu.

Here, for simplicity, we will not be concerned with the mechanism of the isotropic hyperfine interaction and assume that the hyperfine mechanism does not change at 1 K. By considering the field only from nearest-neighbour U atoms, we define rather arbitrarily the isotropic field at a Cu site as

$$\boldsymbol{H}_{\mathrm{iso}} = \alpha \sum_{\mathrm{NN}} \boldsymbol{H}(m_j, r_j) \equiv \alpha \boldsymbol{M}_{\mathrm{eff}} \tag{12}$$

where $\boldsymbol{H}_j(m_j, r_j)$ is the field produced by the jth U atom, α is treated as a parameter that depends on the crystallographic site and the sum is taken over only nearest-neighbour U atoms. $\boldsymbol{M}_{\mathrm{eff}}$ is the effective magnetization vector at the nuclear site defined for convenience. Here, we only consider the magnetic symmetry of Cu sites and are not concerned with the origin of the hyperfine mechanism, i.e. the value of α. For UCu_5, the number of nearest-neighbour magnetic atoms is four for the 4c site and three for the 16e sites. The local symmetry of both sites is schematically shown in figure 11. In the following discussion, local coordinate systems are taken as the indication in the figure. Although we cannot deduce from our model any information on the absolute value of the hyperfine interaction, the model is expected to be reliable for the symmetry consideration.

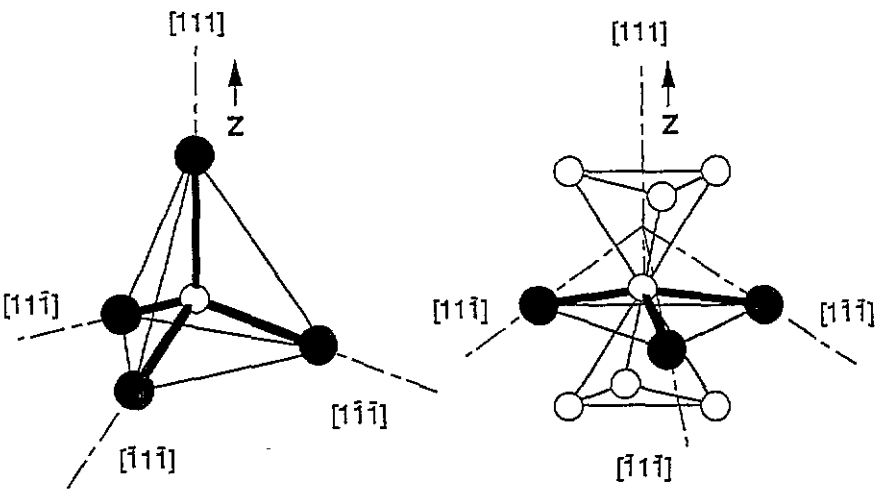

Figure 11. Local symmetry of Cu sites: left, 4c site; right, 16e site. Open and full circles represent Cu and U atoms, respectively.

5.1.2. Expected magnetic sites of Cu. Assuming the 1-q and 4-q antiferromagnetic structures, we will calculate local fields at nuclear sites. We define the isotropic hyperfine coupling vector A_{iso} as

$$H_{iso} \equiv m_0 A_{iso} \tag{13}$$

where m_0 is the magnitude of the ordered moment. Using equation (12), we have

$$A_{iso} = \alpha M_{eff}/m_0. \tag{14}$$

For Cu sites in the 1-q and 4-q structures, we find several magnetic sites with different magnetic local symmetry, which are schematically shown in figure 12. Notation of the magnetic sites is given in the figure. The calculated values of $A_{iso} = |A_{iso}|$ and the angles between A_{iso} and the local symmetry axis are listed in table 1. Since we do not know the absolute value of A_{iso}, we list only the ratio within each crystallographic site. The values of the 4c-II and 16e-II sites in the 1-q structure were taken to be unity. The symmetry axes were taken as in figure 11, and the sign was taken so that the projection of M_{eff} on the principal axis becomes positive. Then, the signal of A_{iso} should be negative if the hyperfine field at a given nuclear site is antiparallel to M_{eff} and vice versa.

Table 1. Magnetic Cu sites and calculated hyperfine coupling constants in the 1-q and 4-q structures in figure 1. For details see text.

Magnetic structure	Crystallographic site	eq [a]	Magnetic site	A_{iso} (au)	θ_{iso} [b] (deg)	A_{dip} (kOe μ_B^{-1})	θ_{dip} [b] (deg)	Number[c]
4-q	4c	0	4c-I	0	—	0	—	1
			4c-II	1	54.7	−1.718	54.7	3
	16e	≠0	16e-I	0.52	0	−0.864	0	4
			16e-II	1	29.5	−1.125	48.7	12
1-q	4c	0	4c-II	0.86	0	−1.148	0	4
	16e	≠0	16e-I	1.51	0	−1.545	0	4
			16e-II	0.52	70.5	+0.878	85.8	12

[a] The maximum component of the electric field gradient.
[b] Local coordinates were taken to be $\cos\phi > 0$, where ϕ is the angle between M_{eff} and the local principal axis (see figure 12).
[c] The number of atoms among 20 Cu atoms in the crystallographic unit cell.

For the dipole field, m_j in equation (11) is replaced by $m(r)$ in equation (3). Since, in our models, the magnitude of magnetic moment is the same for all U sites, we introduce the relation

$$m_j = m_0 \sum_i \frac{m_i}{m_0} \exp(2\pi i q_i \cdot R_j) \tag{15}$$

where R_j is the radial vector from a given U atom to the jth U atom, and the summation is taken over all q_i components. Then, the dipole field is rewritten as

$$H_{dip} = m_0 \sum_j \sum_i \hat{A}_{dip} \frac{m_i}{m_0} \exp(2\pi i q_i \cdot R_j) \equiv m_0 A_{dip} \tag{16}$$

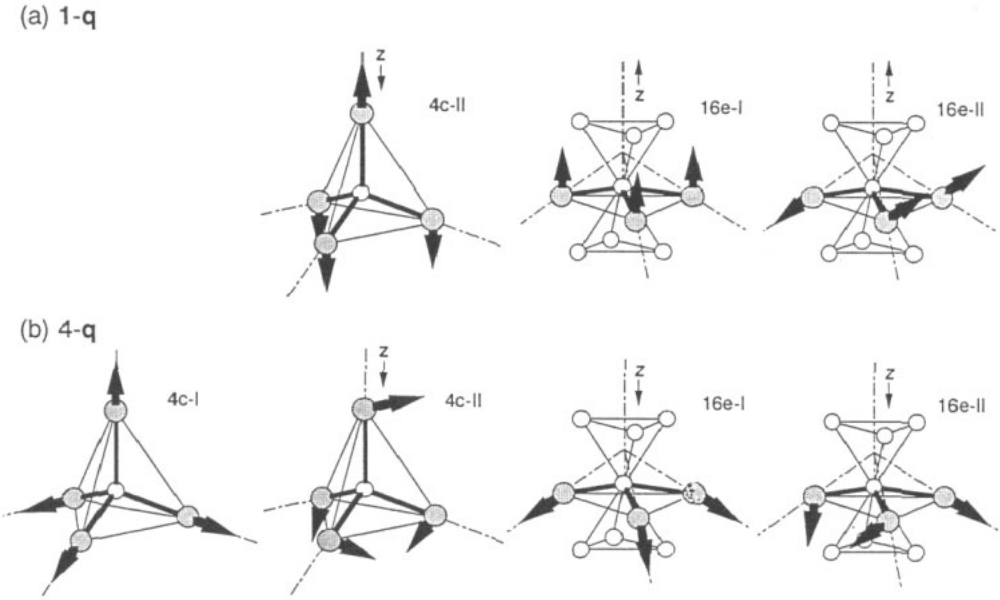

Figure 12. Magnetic local symmetry around Cu sites: (*a*) 1-*q* structure; (*b*) 4-*q* structure. Open and hatched circles represent Cu and U atoms, respectively. The sites with opposite spin directions also belong to the same sites.

where $\hat{A}_{dip}$ is a tensor and A_{dip} a vector field describing the dipole hyperfine coupling. We calculated the dipolar field tensor over a sphere of radius 10 times the lattice constant. The lattice parameter at room temperature was used. The calculated values of $A_{dip} = |A_{dip}|$ and the angles between A_{dip} and the local symmetry axis are tabulated in table 1. Crystallographic Cu sites separate into several magnetic sites, which correspond to the sites distinguished by the isotropic field.

The position of the separated magnetic sites in a crystallographic unit cell is schematically shown in figure 13. For the 1-*q* structure, the 4c site remains equivalent in the ordered state, while for the 4-*q* structure, the 4c site separates into two magnetic sites. It should be noted that, in the 4-*q* structure, the hyperfine field cancels at a part of the 4c site (4c-I site), while in the 1-*q* structure, all of the 4c site feels a finite hyperfine field. This implies that these two structures can be distinguished by checking the presence of the Cu NMR signal with $K \sim 0$. The directions of the isotropic and dipole fields are parallel or antiparallel for the 4c-II sites. For both structures, the 16e site separates into two magnetic sites with the number in the ratio 1:3. Although we cannot estimate the absolute values of A_{iso}, an appreciable difference of the relative values depending on the magnetic structure should be noted. The relative values will be compared with experimental results in section 5.2.

5.1.3. Magnetic structures above and below 1 K. It is unambiguous that both high-temperature and low-temperature states are antiferromagnetically ordered states. In order to determine the magnetic structures, essential experimental results are reviewed.

(i) Neutron diffraction measurement by Schenck *et al* (1990) revealed that the magnetic

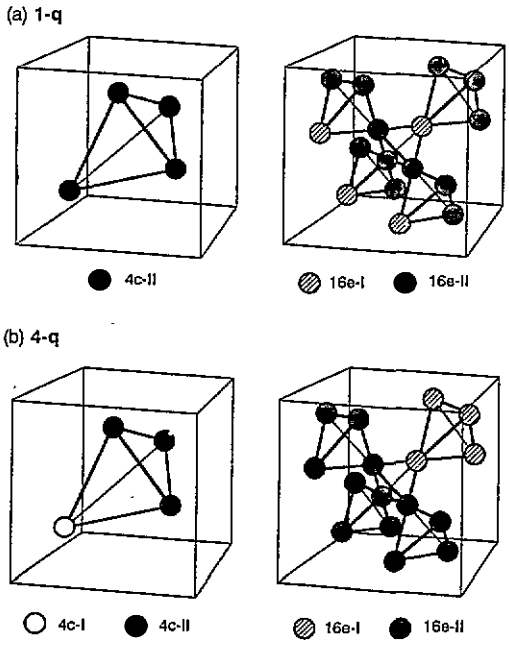

Figure 13. Magnetic Cu sites of UCu_5 assuming the 1-q and 4-q structures in figure 1. Magnetic cell is just taken as figure 1.

scattering does not change above and below 1 K. Therefore, as discussed in section 2, only two magnetic structures are possible for both states above and below 1 K.

(ii) In the NMR measurement, the resonance with $K \sim 0$ was observed between 15 and 1 K. This contradicts with the 1-q structure.

(iii) The resonance with $K \sim 0$ disappears below 1 K and the zero-field NMR spectrum is discontinuously modified at 1 K.

Following the discussion in the previous section, it is natural to conclude that the magnetic structure between 15 and 1 K is the 4-q structure, which transfers to the 1-q structure at 1 K. This model explains simultaneously neutron diffraction and NMR results. Experimentally, this conclusion is undoubted provided that our basic assumption in selecting the candidates of magnetic structure are justified.

Complicated multiple-q structures have been found in several rare-earth and uranium compounds. The structure above 1 K is, however, the first example of the 4-q structure of type-II antiferromagnets, which is experimentally evidenced to be actually present as far as we know. The anomalous macroscopic properties of UCu_5 such as the SDW-like electrical resistivity and metamagnetic-like magnetization may be related with the complicated non-collinear structure. Recently, Yamagishi *et al* (1992) measured the magnetization of UCu_5 using a pulsed magnetic field up to 40 T with temperatures ranging from 1.3 to 15 K. They obtained complicated multi-step magnetization curves and proposed a magnetic phase diagram. The result was explained in terms of our model of the magnetic structure. This strongly supports our discussion. In the next section, we try to explain the complicated zero-field spectra assuming the magnetic structures determined in this section.

5.2. Analysis of zero-field spectra

In the spectra in figure 8, several pairs of peaks corresponding to ^{63}Cu and ^{65}Cu resonances are seen. A discontinuous variation at 1 K strongly suggests that the transition is of spin structure. Here, we try to interpret the spectra assuming the respective structures concluded in the previous section. Especially, we will estimate the isotropic hyperfine coupling constants for both 4c and 16e sites in both high-temperature and low-temperature states, which will be compared with our model described in section 5.1.2.

5.2.1. The 4c site. As shown in table 1, in the 4-q structure, the 4c site separates into two magnetic sites and three-quarters of the 4c site, which is denoted as 4c-II site, feels a finite local field. On the other hand, in the 1-q structure, the 4c site remains equivalent and all of the site, which is also denoted as 4c-II site for convenience, feels a finite local field. It is easy to assign these sites because of the absence of the quadrupole effect due to its cubic symmetry. The ^{63}Cu and ^{65}Cu signals from these sites should satisfy the following two conditions. (i) The ratio of resonance frequencies of ^{63}Cu and ^{65}Cu agrees with $^{63}\gamma/^{65}\gamma = 0.9335$. (ii) The ratio of the nuclear magnetic relaxation rates of ^{63}Cu and ^{65}Cu agrees with $(^{63}\gamma/^{65}\gamma)^2 = 0.8714$, provided that the relaxation is dominated by the magnetic hyperfine interaction. By checking these two ratios, we confirmed that only signals marked by arrows in figure 8 can be assigned to the 4c-II site (see table 2). From the resonance frequencies, we can estimate the magnitude of local field H_{loc}, whose temperature dependence was presented in figure 9. It should be noted that the magnitude reduces below 1 K. The hyperfine coupling constant in the magnetically ordered state is formally calculated by assuming a simple relation such as

$$H_{loc} = m_0 A_{loc}. \tag{17}$$

Here, we use $m_0 = 1.55\mu_B$ obtained by the most recent neutron diffraction experiment for both high-temperature and low-temperature states (Schenck *et al* 1990). Thus, the hyperfine coupling constants are estimated to be

$$|A_{loc}(4q)| = 7.39 \text{ kOe } \mu_B^{-1} \qquad \text{and} \qquad |A_{loc}(1q)| = 6.16 \text{ kOe } \mu_B^{-1}$$

for the 4c-II site in the 4-q structure above 1 K and in the 1-q structure below 1 K, respectively. These values are much larger than the calculated dipole field (see table 1). Therefore, the hyperfine field is mainly produced by the isotropic mechanism.

Table 2. Assignment of the 4c-II site.

Temperature (K)	1.4	0.8
Magnetic structure	4-q	1-q
Cu site	4c-II	4c-II
Resonance frequency (MHz)		
^{63}Cu	12.92	10.78
^{65}Cu	13.84	11.55
frequency ratio	0.934	0.933
H_{loc} (kOe)	11.45	9.55

The directions of isotropic and anisotropic fields should be parallel or antiparallel as was mentioned in section 5.1.2. The sign of coupling depends on the isotropic hyperfine mechanism. Thus, a relation

$$|A_{iso}| \pm |A_{dip}| = |A_{loc}| \tag{18}$$

should hold. It should again be worth while noting that the NMR signal of the 4c-I site in the 4-q structure shows a negative shift by applying an external field (see figure 7). This suggests that, when the ordered moments tilt from the equilibrium direction by applying a field and, as a result, the effective magnetization at the nuclear site increases, the 4c-I site feels a negative hyperfine field. This implies that the isotropic hyperfine coupling constant of the 4c-I site is negative. Therefore, it is reasonable to consider that the isotropic hyperfine constants are also negative for the other Cu sites. Thus, assuming negative A_{iso} and using the calculated values of dipole fields and experimental values of local fields, we obtain

$$A_{iso}(4q) = -8.57 \text{ kOe } \mu_B^{-1} \qquad \text{and} \qquad A_{iso}(1q) = -7.31 \text{ kOe } \mu_B^{-1}$$

for the 4-q and 1-q structures, respectively. The ratio $A_{iso}(1q)/A_{iso}(4q) = 0.85$ is compared with the calculated value assuming the simple model, i.e. 0.86 (see tables 1 and 5). The agreement is excellent in spite of the simplified model. This is not surprising because the 4c site is located at a high-symmetry position and the ratio does not depend on the hyperfine mechanism but only on the magnetic symmetry. This result clearly indicates that the reduction of the hyperfine field at the 4c site below 1 K is reasonably interpreted in terms of only the reorientation of the ordered spin.

5.2.2. The 16e site. For both 1-q and 4-q structures, the 16e sites separates into two magnetic sites with the number in the ratio 1:3. We denote minority and majority sites 16e-I and 16e-II, respectively. It is rather difficult to analyse the resonance from these sites because of the coexistence of the Zeeman and quadrupolar interactions with comparable magnitude. We analyse the spectrum by solving numerically the secular equation for the following Hamiltonian. The Hamiltonian including the Zeeman and quadrupole terms for nuclear spin $I = 3/2$ in the local symmetry of $\eta = 0$ is

$$AI_z + B(3I_z^2 - \tfrac{15}{4}) + C[I_z(I_+ + I_-) + (I_+ + I_-)I_z] + D(I_+^2 + I_-^2) \tag{19}$$

where

$$A = \gamma\hbar H \qquad C = \tfrac{1}{4}h\nu_Q \sin\theta\cos\theta$$

$$B = \tfrac{1}{12}h\nu_Q(3\cos^2\theta - 1) \qquad D = \tfrac{1}{8}h\nu_Q \sin^2\theta$$

and θ is the angle between the direction of magnetic field H and the local symmetry axis and ν_Q is the quadrupole frequency given by equation (9). In this analysis, the field H consists only of the internal field H_{loc}. The value of ν_Q depends on the kind of nucleus, i.e. ^{63}Cu and ^{65}Cu, but is given by a unique parameter, the EFG at the 16e site,

$$eq = \frac{2h}{e}\frac{^{63}\nu_Q}{^{63}Q} = \frac{2h}{e}\frac{^{65}\nu_Q}{^{65}Q} \tag{20}$$

where quadrupole moments ^{63}Q and ^{65}Q are -0.211 and -0.195 barn, respectively. By treating H, θ and eq as parameters and solving the secular equation numerically, we

calculate resonance frequencies of transitions between obtained eigenstates. The intensity of the signal, i.e. transition probability between mth and nth eigenstates, is calculated using the obtained wavefunctions, $I \propto |\langle m|I_x|n\rangle|^2$. Here, we try to assign only the majority 16e-II site, because the resonance lines from the minority site are not well resolved due to the small intensity. The analysis was carried out in the following manner. Six main peaks except those assigned to the 4c-II site were selected (three for ^{63}Cu and three for ^{65}Cu). Although the other small peaks should correspond to the resonance from the minority 16e-I site, we will not consider them. Using some trial values of H and θ and experimental values of ν_Q obtained by the NQR measurements, we found the correspondence of experimental resonances to transitions between obtained eigenstates. After that, by varying all three parameters H, θ and eq, the best-fit values were sought to minimize

$$R = \sum_{i=1}^{6} |\nu_i^{\mathrm{exp}} - \nu_i^{\mathrm{cal}}|^2 \tag{21}$$

where ν_i^{exp} and ν_i^{cal} mean the experimental and calculated resonance frequencies of ith transition, respectively. We were not concerned with the signal intensity in this analysis because the frequency dependence of sensitivity of the spectrometer was not calibrated in the experiment. The best-fit results are shown by lines in figure 8. Numerical results of the calculated resonance frequencies are listed in table 3 together with corresponding experimental frequencies. The fitting is excellent and the fitting error is within 0.3%. The local field and the EFG at the 16e-II site estimated in this analysis are presented in table 4. It is notable that every parameter changes considerably at 1 K. The hyperfine coupling constant defined by equation (17) is

$$|A_{\mathrm{loc}}(4\mathrm{q})| = 9.48 \text{ kOe } \mu_{\mathrm{B}}^{-1} \qquad \text{and} \qquad |A_{\mathrm{loc}}(1\mathrm{q})| = 7.17 \text{ kOe } \mu_{\mathrm{B}}^{-1}$$

for the 4-q and 1-q structures, respectively. Similarly to the 4c-II site, much larger values than the estimated dipole field were obtained, which indicates the dominance of the isotropic field.

Table 3. Experimental resonance frequencies for the 16e-II site and calculated ones using best-fit values of H, θ and eq in table 4.

	1.4 K		0.8 K	
	ν^{exp} (MHz)	ν^{cal} (MHz)	ν^{exp} (MHz)	ν^{cal} (MHz)
^{63}Cu	14.26	14.24	8.52	8.53
	18.50	18.52	14.22	14.26
	20.86	20.85	18.43	18.38
^{65}Cu	15.80	15.79	9.49	9.45
	19.18	19.21	14.78	14.76
	21.46	21.45	18.90	18.93

The angle θ changes from $\sim 50°$ above 1 K to $\sim 80°$ below 1 K (see table 4). According to our very simple model, the angle between the isotropic field on the 16e-II site and its local symmetry axis changes from $\sim 30°$ to $\sim 70°$ with the magnetic structure changing from 4-q to 1-q (see table 1). The trends are in fairly good agreement with each other. The small difference between them can be ascribed to the contribution of the dipole field.

Table 4. Hyperfine field and electric field gradient at the 16e-II site.

Temperature (K)	1.4	0.8
Magnetic structure	4-q	1-q
Cu site	16e-II	16e-II
H_{loc} (kOe)	14.70	11.11
θ (deg)	50.36	77.21
$^{63}\nu_Q$ (MHz)[a]	12.80	13.70

[a] ^{63}Cu quadrupole frequency is represented for the electric field gradient.

Table 5. Experimental and calculated isotropic hyperfine coupling constants for the 4c-II and 16e-II sites.

Magnetic Cu site	Magnetic structure	Experiment (kOe μ_B^{-1})	Experiment ratio	Calculation ratio
4c-II	4-q	−8.57	1	1
	1-q	−7.31	0.85	0.86
16e-II	4-q	−7.80	1	1
	1-q	−4.56	0.57	0.52

If we use the model of the hyperfine mechanisms described in section 5.1.1, the following relation should hold for the projected component of the hyperfine field on the local principal axis:

$$|A_{iso}| \cos\theta_{iso} \pm |A_{dip}| \cos\theta_{dip} = |A_{loc}| \cos\theta_{exp} \tag{22}$$

where θ_{iso}, θ_{dip} and θ_{exp} are the angles between the local symmetry axis and the isotropic, dipole and observed fields, respectively. The $\pm$ sign corresponds to the fact that the direction of the coupling between isotropic and anisotropic fields is not known. If we assume that the isotropic hyperfine coupling constant is negative by referring to the discussion for the 4c-II site, we can estimate the isotropic hyperfine constants at the 16e-II site using experimental values A_{loc} and θ_{exp} and calculated values θ_{iso}, A_{dip} and θ_{dip}. They are

$$A_{iso}(4q) = -7.80 \text{ kOe } \mu_B^{-1} \qquad \text{and} \qquad A_{iso}(1q) = -4.56 \text{ kOe } \mu_B^{-1}$$

for the 4-q and 1-q structures, respectively. The ratio of the hyperfine coupling constants is tabulated in table 5. The agreement between the experiment and calculation is fairly good in spite of the lower symmetry of the 16e site than the 4c site. This justifies our simple model of the hyperfine mechanism and the conclusion concerning the magnetic structures.

5.2.3. Information from zero-field spectra. The main results obtained in the analysis of the zero-field spectra are summarized below.

(i) The local field at Cu sites is mainly produced by the isotropic mechanism. At both 4c-II and 16e-II sites, the local field is reduced below 1 K. The direction of the local field at the 16e-II site changes from $\theta \sim 50°$ above 1 K to $\theta \sim 80°$ below 1 K. This apparently indicates that the direction of U moment is modified at 1 K. The reduction of the field and the variation of the angle are reasonably explained in terms of the spin reorientation from 4-q to 1-q structures.

(ii) The EFG, which is proportional to ν_Q, does not change substantially at 15 K, while it changes considerably at 1 K (see table 4 and figure 5). This indicates that the transition at 15 K is rather conventional, while that at 1 K is anomalous, accompanied by the variation of the local electrostatic environment.

We did not find any inconsistency between our model of spin structures and the experimental results. In addition, interesting information on the electronic state was deduced from the analysis. It is notable that the variation of magnetic parameters at 1 K is well explained by a very simple and rather classical picture.

5.3. Nature of the transition at 1 K

If the spatial distribution of the 5f wavefunction interacts with the electrostatic potential, in the ordered state, and if the electrostatic interaction competes with the exchange interaction, a non-collinear antiferromagnetic structure, which may be called the quadrupole ordering, is realized to minimize the electrostatic energy. The 4-q structure of UCu_5 may be the case. The stability of the structure should be related to the magnetic symmetry and the large degeneracy of the crystal-field state of U ions in the high-symmetry (FCC) lattice. Some uranium and rare-earth compounds exhibit a similar transition of the magnetic structure from 1-q to multiple-q structures, the origin of which is usually ascribed to the conversion of crystal-field state and the interaction with quadrupole moments. The transition temperature is usually of the order of 10–100 K. Since the crystal-field splitting was not observed for UCu_5 by inelastic neutron scattering, the classical local-moment picture seems to be irrelevant. Furthermore, the transition temperature is extremely low, 1 K, which is too low to be explained by the crystal-field energy. Therefore, it seems that a new concept is necessary to explain the stability of the 4-q structure as well as the origin of the transition at 1 K.

The nuclear spin–lattice relaxation rate, $1/T_1$, for ^{63}Cu is discontinuously reduced by about two orders of magnitude at 1 K (Nakamura *et al* in preparation). This proves from a microscopic viewpoint the reduction of the density of states at the Fermi level, i.e. energy-gap formation in the spin excitation spectrum. Thus, UCu_5 provides an example of a heavy-fermion state with an energy gap and, at the same time, an antiferromagnetic state with a fairly large ordered moment of the order of $1\mu_B$. The energy-gap formation was found in several Kondo lattice systems (see, for example, Fisk and Aeppli 1992, Kasuya 1993). Although the origin of the gap formation is still controversial, the gap state draws much interest as one of the unique states that may originate from the hybridization effect between f and conduction electrons. The gap state in UCu_5 should be classified in the same category as other dense Kondo substances; then the origin should be interpreted in terms of the same context.

The variation of the averaged magnetic parameters at 1 K is described by the rather classical picture, i.e. only the spin reorientation. The fact that the hyperfine fields can be described by the same mechanism for both high-temperature and low-temperature states suggests that the hyperfine interaction is dominated by the direct mixing of U 5f and Cu wavefunctions because, if the hyperfine interaction is mediated by only the conduction-electron polarization, the hyperfine mechanism is expected to be markedly modified by the gap formation at the Fermi level. On the other hand, the most important characteristic of the transition at 1 K is the considerable change of electrostatic parameter, ν_Q (see table 4 and figure 5). The EFG in metallic compounds consists of ionic and electronic contributions coming from the ionic charge on all the other lattice sites around the nucleus of interest and the intra-atomic charge distribution, respectively,

$$eq = eq^{\text{lat}}(1 - \gamma_\infty) + eq^{\text{elec}} \tag{23}$$

where γ_∞ is the Sternheimer antishielding factor, which arises from the charge redistribution of core electrons induced by the charge of the surrounding ions (Sternheimer 1954). The

lattice term is related to the unit-cell volume since it is a function of the interatomic distance. On the other hand, the electronic term depends strongly on the spatial distribution of Cu wavefunctions, which are expected to be modified significantly by the hybridization with conduction electrons or by the redistribution via the exchange interactions with U 5f or conduction electrons. The high-temperature variation of ν_Q of UCu_5 may be ascribed to the change of lattice term associated with thermal expansion. For UCu_5, the lattice volume change was not observed at 1 K by neutron diffraction measurement within experimental accuracy (Schenck *et al* 1990). Therefore, the discontinuous change of ν_Q at 1 K may be ascribed mainly to the variation of the electronic term associated with the redistribution of Cu wavefunctions caused by energy-gap formation. An alternative interpretation is the symmetry breaking of lattice or charge distribution. The transition from the 4-q structure with cubic symmetry to the 1-q structure with trigonal symmetry may induce small crystal distortion by, for example, a Jahn–Teller mechanism, which may be too small to be detected by neutron diffraction. The transition of charge distribution such as a charge ordering and charge-density wave is also a possible origin. In the present stage, symmetry breaking is evidenced in neither crystal structure nor charge distribution. Therefore, experiments to detect such variations may be interesting.

Finally, the origin of the spin reorientation is considered. Being associated with the gap formation, the exchange interaction between U moments would be markedly modified. Especially, the reduction of conduction-electron concentration at 1 K would be responsible for the variation of the exchange interaction. As a result, the direction of spin may be modified. In this case, the anisotropy of exchange interaction, which was neglected in our analysis, should be important. Alternatively, the spatial redistribution of the 5f-electron wavefunction itself would considerably modify the interaction of the multipole moment with the crystal field. Naively, it may be considered that, in the strongly localized state with energy gap, the exchange interaction having a preference for a collinear arrangement prevails over the electrostatic energy to stabilize the collinear 1-q structure below 1 K. The nature of the transition at 1 K, which is rather conventional in a magnetic viewpoint and unconventional in an electrostatic viewpoint, seems to support the latter interpretation. Anyhow, the gap formation should be a result of the many-body effect being a characteristic of the strongly correlated electron systems. It seems that the complete understanding of the origin of the gap formation has critical significance to progress the physics of strongly correlated electron systems.

6. Conclusion

We have measured Cu NMR and NQR of the heavy-fermion antiferromagnet UCu_5 in the paramagnetic and magnetically ordered states. It was revealed from the analysis of the NMR spectrum that the spin structure between 15 and 1 K is the non-collinear 4-q structure, which is different from the collinear 1-q structure proposed previously by Murasik *et al* (1974). In addition, we showed unambiguously that the 4-q structure transfers to the 1-q structure at 1 K. It is notable that both structures do not lead to any difference in the neutron diffraction pattern and were distinguished, for the first time, by our NMR study. Assuming a simple model for the hyperfine mechanism, the complicated zero-field spectra for both states were consistently reproduced by using the above picture of the transition. The gap state is classified as the exotic state induced in the antiferromagnetic heavy-fermion state.

A theoretical calculation of electron polarization at Cu sites and a theory dealing with the stability of the magnetic structures are strongly hoped for. Experiments using a single crystal are expected to progress considerably the physics in UCu_5.

Acknowledgments

One of the authors (HN) would like to thank Dr S Kawarazaki at Osaka University for helpful discussions about neutron diffraction and magnetic structures and Ms M Inoue for assistance with experiments.

References

Baenziger N C, Rundle R E, Snow A I and Wilson A S 1950 *Acta Crystallogr.* **3** 34
Barth S R, Ott H R, Gygax F N, Schenck A, Rice T M and Fisk Z 1986 *Hyperfine Interact.* **31** 397
Brodsky M B and Bridger N J 1973 *Magnetism and Magnetic Materials (AIP Conf. Proc. 18)* ed C D Graham Jr and J J Rhyne (New York: American Institute of Physics) p 357
Buschow K H J, Locher P R and Leger M 1979 *J. Phys. F: Met. Phys.* **9** 2483
Carter G C, Bennett L H and Kahan D J 1977 *Metallic Shifts in NMR (Prog. Mater. Sci. 20)* (Oxford: Pergamon)
Chakravarthy R, Paranjpe S K, Murthy M R L N, Madhav Rao L and Satya Murthy N S 1985 *Phys. Status Solidi* a **88** K155
Coldea M and Pop I 1985 *J. Magn. Magn. Mater.* **47/48** 555
Coldea M, Pop I, Wallace W E and Narasimham K S V L 1976 *Magn. Lett.* **1** 11
Fisk Z and Aeppli G 1992 *Comments Condens. Matter Phys.* **16** 155
Grohs H, Höchst H, Steiner P, Hüfner S and Buschow K H J 1980 *Solid State Commun.* **33** 573
Herrmann-Ronzaud D, Burlet P and Rossat-Mignod J 1978 *J. Phys. C: Solid State Phys.* **11** 2123
Kasuya T 1993 *Japan. J. Appl. Phys. Ser.* **8** 3
Misiuk A, Mulak J and Czopnik A 1973 *Bul. Acad. Polon. Sci., Ser. Sci. Chim.* **21** 487
Murasik A, Ligenza S and Zygmunt A 1974 *Phys. Status Solidi* a **23** K163
Nakamura H, Kitaoka Y, Asayama K and Ōnuki Y 1991 *Physica* **171B** 329
Nakamura H, Kitaoka Y, Inoue M, Asayama K and Ōnuki Y 1990 *J. Magn. Magn. Mater.* **90/91** 459
Nakamura *et al* 1994 in preparation
Ōnuki Y, Yamazaki T, Ukon I, Komatsubara T, Sato H, Sugiyama Y, Sakamoto I and Yonemitsu K 1989a *J. Physique Coll.* **49** C8 481
Ōnuki Y, Yamazaki T, Ukon I, Komatsubara T, Umezawa A, Kwok W K, Crabtree G W and Hinks D G 1989b *J. Phys. Soc. Japan* **58** 2119
Ott H R, Rudigier H, Felder E, Fisk Z and Batlogg B 1985 *Phys. Rev. Lett.* **55** 1595
Rossat-Mignod J 1987 *Methods of Experimental Physics* vol 23, part C (Orlando, FL: Academic) p 69
Roth W L 1958 *Phys. Rev.* **111** 772
Schenck A, Birrer P, Gygax F N, Hitti B, Lippelt E, Weber M, Böni P, Fischer P, Ott H R and Fisk Z 1990 *Phys. Rev. Lett.* **65** 2454
Sternheimer R M 1954 *Phys. Rev.* **95** 736
Takagi S, Homma T and Kasuya T 1989 *J. Phys. Soc. Japan* **58** 4610
van Daal H J, Buschow K H J, van Aken P B and van Maaren M H 1975 *Phys. Rev. Lett.* **34** 1457
van Laar 1965 *Phys. Rev.* **138** A584
Walter U, Loewenhaupt M, Holland-Moritz E and Schlabitz W 1987 *Phys. Rev.* B **36** 1981
Yamagishi A, Senda K, Kindo K, Date M and Ōnuki Y 1992 *J. Magn. Magn. Mater.* **108** 211
Zołnierek Z, Troć R and Kaczorowski D 1987 *J. Magn. Magn. Mater.* **63/64** 184